EUSIPCO 2013 1569743905

NON-UNIFORM SPECTRUM SENSING FOR COGNITIVE RADIO USING SUB-NYQUIST SAMPLING

Babar AZIZ, Samba TRAORÉ and Daniel LE GUENNEC

IETR / SUPELEC, Campus de Rennes Avenue de la Boulaie - CS 47601
F-35576 Cesson-Sevigne cedex, France
Email: {babar.aziz,samba.traore,daniel.leguennec}@supelec.fr

ABSTRACT

Spectrum sensing is the very task upon which the entire operation of Cognitive Radio rests. In this paper, we propose a spectrum sensing technique based on the estimates of the spectrum of a multiband signal obtained from its compressed samples. We show that our proposed spectrum sensing method provides accurate results using less data samples. We also show the effect of false detection on the average sampling rate of a non-uniform sub-Nyquist sampler.

Index Terms— Non-uniform sub-Nyquist sampling, Cognitive radio, Spectrum sensing.

1. INTRODUCTION

The available electromagnetic radio spectrum is a precious but limited natural resource. Moreover, the licensed part of the radio spectrum is not efficiently used, as the license cannot change the type of use or transfer the right to other licensee. Due to this current static licensing approach of spectrum, spectrum holes or spectrum opportunities arise. Cognitive Radio (CR), a new way of looking at wireless communications, has the potential to become the solution to the spectrum under utilization problem, by allowing unlicensed users, to access these spectrum holes for transmission [1, 2]. The first cognitive task is to develop wireless spectral detection and estimation techniques for sensing the available spectrum. Spectrum sensing can be defined as the task of detecting the presence or absence of a signal by sensing the radio spectrum. Some popular spectrum sensing techniques are energy detection, matched filter and cyclostationary feature detection that have been proposed for narrow band sensing [3]. All these techniques function by filtering the received signal with narrowband band-pass filters and then sample it uniformly at the Nyquist rate. In these approaches to spectrum sensing, the detection process boils down to a binary hypothesis-testing problem i.e. to detect presence (H_1) or absence (H_0) of a primary user in the considered band.

As it is well known that with the advances in wireless communications, future cognitive radios should be capable of scanning a wideband of frequencies, in the order of few GHz. The usual sampling of a wideband signal needs high sampling rate ADCs, which need to operate at or above the Nyquist rate. The above mentioned spectrum sensing techniques have their respective advantages and disadvantages over one another. But a common drawback is that they operate at Nyquist sampling rate. Since, sampling a wideband at Nyquist rate followed by the processing of huge amount of sampled data in real time requires a lot of effort and poses a major implementation challenge.

To overcome this problem, solutions based on compressive sampling have been proposed in [4–6]. In [4], the signal is detected from the estimated spectrum obtained from the compressed samples of the signal. However, spectrum estimation of a signal from its compressed samples is achieved by solving an optimization problem, which is not an easy task. By using the fact that the wireless signals in open-spectrum networks are typically sparse in the frequency domain, in [6], a sensing method based on MUSIC algorithm has been proposed. This sensing method is of particular interest as it is implemented for a sub-Nyquist sampling technique known as the Multi-Coset (MC) sampling. Authors in [6] claim that the proposed method would bring substantial saving in terms of the sampling rate. However, the performance of the proposed method degrades at low SNRs and also requires more data samples to correctly detect the signal. An improved version of [6] is presented in [7], which works well at low SNRs but at the cost of high complexity.

In this paper, based on the sparsity of the multiband signals in frequency domain and using non-uniform sub-Nyquist sampling of the input signal, we propose a wideband spectrum sensing method for the detection of active bands that would bring substantial saving in terms of the sampling rate. The performance of the proposed method is examined at low SNR values with less data samples and is found to produce accurate results. In the next section the system model is presented and in Section 3 the non-uniform spectrum sensing method is presented and the functionality of each block in the model is explained. Simulation results are shown in Section 4 and finally conclusion is drawn in Section 5.

2. SYSTEM MODEL OF NON-UNIFORM SAMPLER

One of the main objectives of Software Radio (SR) is to propose new technologies to design wireless infrastructure able to support multi-service, hardware-independent operations [2]. Furthermore, CR continues to gain popularity as it adapts intelligently to the radio environment by dynamically managing the spectrum and, therefore, results in a spectrum which changes continuously [2]. Keeping the aspects of SR and CR in mind, we have proposed a sampling system, that adapts to the changes in the input signal spectrum and is not constrained by the inflexibility of hardwired circuitry. We call it the *Dynamic Single Branch Non-Uniform Sampler* (DSB-NUS) or simply the DSB sampler [8], see Fig. 1. DSB sampler is based on the principle of MC sampling except that instead of p input branches in case

of MC sampling, the DSB sampler has only one input branch. Furthermore, in the DSB sampler, an adaptation loop is introduced which dynamically measures the spectral support of the input signal from time to time, to adapt the sampling rate according to the spectrum of the input signal i.e. reducing the sampling rate if the signal sparsity in frequency domain is high and vice versa. The traditional MC sampling lacks this adaptive, feed-back mechanism and is rather a static, hardwired system. In this paper, we focus on the spectrum sensing method used in the DSB sampler. Since, the working of the DSB sampler is not the subject of this paper, here we give an overview of the system before presenting our non-uniform spectrum sensing method.

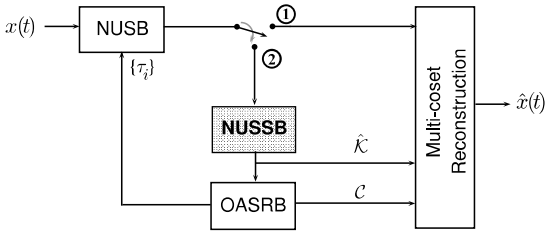

Fig. 1. Dynamic Single Branch Non-Uniform Sampler system.

In DSB sampler, the Non-Uniform Sampler Block (NUSB) performs the non-uniform sub-Nyquist sampling of the input signal $x(t)$. In random sampling, the set of sampling instants $\{t_n\}_{n\in\mathbb{Z}}$ should be different from the set of uniform sampling instants $\{nT\}$ for an average sample period T and $n \in \mathbb{Z}$. The digital signal obtained is given by

$$x_s(t) = \sum_{n=-\infty}^{+\infty} x(t_n)\delta(t - t_n) \tag{1}$$

where signal $x(t)$ is from the class of continuous real-valued signals with finite energy and band-limited to a subset $\mathcal{B} = [-\frac{f_{Nyq}}{2}, \frac{f_{Nyq}}{2}]$. Let $\mathcal{F}$ represent the spectral support of the signal such that $\mathcal{F} \subset \mathcal{B}$ and let N_B be the number of bands in the multiband signal. The NUSB of the DSB sampler is designed as an Adaptive Pseudo Random Sampler (APRS) [9,10]. In APRS, the $\mathcal{N}$ sampling instants are defined as:

$$t_m = t_{m-1} + \alpha_m = t_0 + \sum_{i=1}^{m} \alpha_i \tag{2}$$

where $1 \leq m \leq \mathcal{N}$, $E[t_m] = mT$ and $var[t_m] = m\sigma^2 \; \forall \, \mathcal{N} \geq 1$. Note that $\{\alpha_m\}$ is a set of i.i.d random variables with probability density $p_1(\tau)$, mean T and with variance σ^2. Although, the input components in DSB sampler have changed compared to the traditional MC sampler but the signal at the output of the NUSB remains the same as in the case of MC sampling [11]. As a result, for each L uniformly spaced samples in case of Nyquist sampling, we get p non-uniform samples, see Fig.2. The set $\mathcal{T} = \{\tau_i\}_{i=0}^{p-1}$ is composed of the durations between adjacent p samples where $\tau_i = c_{i+1} - c_i$ for $i \neq 0$ and $i \neq p-1$, $\tau_0 = c_1$ and $\tau_{p-1} = (L + c_0) - c_{p-1}$, see Fig. 2. The set $\mathcal{C} = \{c_i\}_{i=0}^{p-1}$ contains p distinct integers from $\mathcal{L} = \{0, 1, ..., L-1\}$. Now (2) can be written as

$$t_m = t_0 + T \sum_{i=0}^{m-1} \tau_i \qquad 1 \leq m \leq p \tag{3}$$

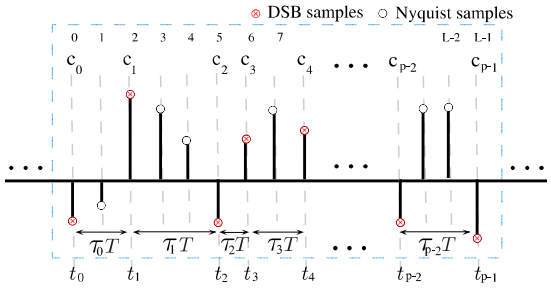

Fig. 2. L uniformly spaced Nyquist samples and corresponding p DSB samples.

The set of sampling instants $\{t_n\}_{n\in\mathbb{Z}}$ is non-uniform and periodic with period L such that $t_p = t_0 + LT$. The DSB sampler adapts its sampling rate according to the sparsity of the spectrum of input signal. Because of this dynamic nature, it needs to calculate and update the parameters $\mathcal{T}$ and $\mathcal{C}$ from time to time to adjust the sampling rate at NUSB. The DSB sampler uses MC reconstruction to reconstruct the input signal. Depending on the application, the reconstruction process in DSB sampler starts by dividing the entire frequency band into L narrowband cells, each of them with bandwidth B, such that $f_{Nyq} = L \times B$ [11]. These cells are indexed from 0 to $L-1$, see Fig. 3. Those spec-

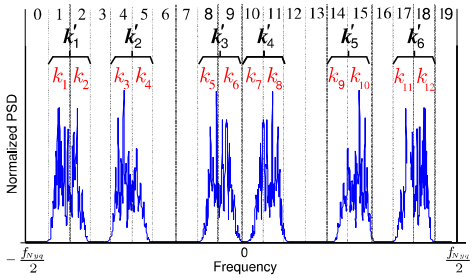

Fig. 3. Division of the observation band into $L = 20$ cells where $\mathcal{K} = \bigcup_{i=1}^{6}\{\boldsymbol{k}_i^{'}\} = \{k_r\}_{r=1}^{12}$ are the indexes of the active cell.

tral cells which contain part of the signal spectrum are called active cells. The indexes of the active cells are collected into a set $\mathcal{K} = \bigcup_{i=1}^{N_B}\{\boldsymbol{k}_i^{'}\} = \{k_r\}_{r=1}^{q}$, called the active cells set. Note that $q = |\mathcal{K}|$ where $|*|$ is the cardinality operator. It can be seen from Fig.3 that the total number of bands in the multiband signal is $N_B = 6$ and the set of active cells indexes is $\mathcal{K} = \{\{\boldsymbol{k}_1^{'}\} \cup \{\boldsymbol{k}_2^{'}\} \cup ... \cup \{\boldsymbol{k}_6^{'}\}\} = \{\{k_1, k_2\} \cup \{k_3, k_4\} \cup ... \cup \{k_{11}, k_{12}\}\} = \{k_1, k_2, ..., k_{12}\}$ and $q = 12$. To perform reconstruction, the number of bands N_B and $\mathcal{K}$ must be known to the MC reconstruction block [11]. These parameters are indispensable to reconstruct the signal but are unknown to the system. Moreover, these parameters are used by the Optimal Average Sampling Rate Block (OASRB) (Fig.1), to update the sets $\mathcal{C}$ and $\mathcal{T}$ which are sent to NUSB, to adapt the sampling rate to the spectrum of input signal, as stated earlier in this section. The DSB sampler basically operates in two phases i.e. the reconstruction phase (switch in position 1) and the adaptation phase (switch in position 2), see Fig. 1. Each time the DSB sampler starts, the switch is in position 2 as the system needs to calculate the parameters $\mathcal{C}, \mathcal{T}$ for the OASRB and $N_B, \mathcal{K}, \mathcal{C}$ for the MC reconstruction

so that it can start sampling according to the spectral content of the signal and can perform reconstruction, respectively. It is the job of the Non-Uniform Spectrum Sensing Block (NUSSB) (shown in bold and shaded in Fig. 1) to compute the parameters N_B and $\mathcal{K}$ from which the parameters $\mathcal{C}$ and $\mathcal{T}$ are computed. Therefore, the NUSSB plays an important role in the operation of DSB sampler.

3. NON-UNIFORM SPECTRUM SENSING BLOCK

Based on the discussion in the previous section, we can re-state the task of the NUSSB as: *Given the observation band,* $\mathcal{B} = [-\frac{f_{Nyq}}{2}, \frac{f_{Nyq}}{2}]$, *the objective is to estimate the active cells set* $\mathcal{K}$ *for optimal reconstruction of the non-uniformly sub-Nyquist sampled signal* $x(t)$. In this section, we present our non-uniform spectrum sensing model. The block diagram of the model is presented in Fig. 4 and the function of each sub block is explained in the next subsections.

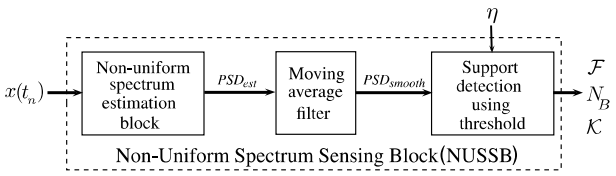

Fig. 4. Non-uniform spectrum sensing model

3.1. Non-uniform spectrum estimation block

As stated earlier, the N_B and the set $\mathcal{K}$ are unknown to the DSB sampler. To find $\mathcal{K}$, two interesting approaches based on MC sampling have been proposed in [6, 7]. However, the MUSIC algorithm based method in [6] shows poor performance at low SNRs and requires more data samples to produce satisfactory results. Authors in [7] proposed an improved version of [6] but it is more complex. Furthermore, the signal $x(t)$ is under sampled and the samples are not evenly spaced, the usual spectrum sensing techniques like energy detection, cyclostationarity cannot be used [3]. In order to overcome this hurdle, we treat this scenario as a *missing data* problem and, in this paper, we propose to use the Lomb-Scargle method [12] to estimate the power spectral density (PSD) of the non-uniformly sampled signal. Then in the remaining sub blocks of the sensing model, N_B and $\mathcal{K}$ are computed from the estimated PSD. The Lomb-Scargle periodogram is a well known tool to detect if an unevenly spaced data is due to noise or it contains also the contribution of a signal by providing an estimate of the PSD. Lomb-Scargle method evaluates the samples, only at times t_n that are actually measured. Suppose that there are N_s samples $x(t_n)$, $n = 1, ..., N_s$. The PSD estimate obtained from Lomb-Scargle method is defined by (4) (spectral power as a function of angular frequency $\omega = 2\pi f > 0$ with $f \in \mathcal{B} = [-\frac{f_{Nyq}}{2}, \frac{f_{Nyq}}{2}]$).

$$PSD_{est} = \frac{1}{2\sigma^2}\left\{\frac{\left[\sum_n (x(t_n)-\overline{x})\cos\omega(t_n-\delta)\right]^2}{\sum_n \cos^2\omega(t_n-\delta)} + \frac{\left[\sum_n (x(t_n)-\overline{x})\sin\omega(t_n-\delta)\right]^2}{\sum_n \sin^2\omega(t_n-\delta)}\right\} \quad (4)$$

where $\overline{x}$ and σ^2 represent the mean and variance of the samples. More detail on Lomb-Scargle method can be found in [12].

3.2. Moving average filter block

It is noted that the PSD estimate obtained from the Lomb-Scargle method has a high variance. As a result of which N_B and $\mathcal{K}$ are not easy to detect if the PSD estimates are used in their original form. Therefore, we use a moving average filter to smoothen the PSD_{est} obtained from the non-uniform sampled data. The moving average filter smooths the incoming PSD_{est} by replacing each data point with the average of the neighboring data points defined within a specified span. In Fig.4, PSD_{smooth} is the smoothed value of the PSD at frequency f. Smoothing is done over a span of $2M + 1$ is the span where M is the number of neighboring data points on either side of PSD_{smooth}. Although this process is simple in operation, but we will show later that the results obtained are quite accurate.

3.3. Support Detector Block

Once a smooth PSD estimate has been obtained, the spectral support $\mathcal{F}$ is computed with reference to a threshold value, η. η is selected dynamically as a function of PSD_{max} i.e. $\eta = \lfloor PSD_{max} - \beta \rfloor$, where β is a fixed value and $\lfloor * \rfloor$ is the floor function. With reference to the threshold η, the number of bands

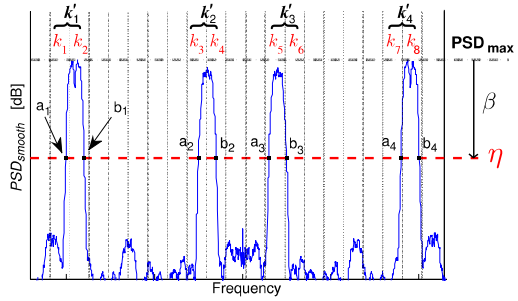

Fig. 5. Support detection using threshold in non-uniform spectrum sensing block.

N_B are computed. The process is illustrated in Fig.5 for a signal with N_B = 4. The spectral support is calculated using the following equation

$$\mathcal{F} = \bigcup_{i=1}^{N_B} [a_i, b_i] \quad (5)$$

where a_i and b_i represent the crossing points at the threshold η, see Fig.5. Once the support $\mathcal{F}$ is found, the set $\mathcal{K}$, can be calculated using (5) as follows

$$\lfloor a_i LT \rfloor \leq \{\boldsymbol{k_i'}\} \leq \lfloor b_i LT \rfloor \quad (6)$$

where $1 \leq i \leq N_B$ and $T = 1/f_{Nyq}$. When all the $\boldsymbol{k_i}$ sets are calculated for each band, the set of spectral indexes $\mathcal{K}$ is computed as

$$\mathcal{K} = \bigcup_{i=1}^{N_B} \{\boldsymbol{k_i'}\} = \{k_r\}_{r=1}^{q} \quad (7)$$

The set $\mathcal{K}$, then, is sent to the OASRSB and MC reconstruction blocks, as shown in Fig.1.

4. NUMERICAL RESULTS

In this section, we present some numerical results for our proposed non-uniform spectrum sensing block (NUSSB). For simulations, the wideband of interest is in the range of $\mathcal{B}$=[-300,300]MHz, therefore, the Nyquist sampling rate is f_{Nyq}=600MHz. We consider a multiband signal with N_B=6 bands, each with a maximum bandwidth of 10MHz. Therefore, the input signal is sparse in the frequency domain. For simplicity we assume that the N_B bands have the same amplitude. 16 QAM modulation symbols are used that are corrupted by the additive white Gaussian noise. Given f_{max} = 300MHz, it is desired to detect N_B and $\mathcal{K}$ for the input signal which is sampled at a sub-Nyquist sampling rate using the DSB sampler. For the NUSSB, β is set equal to 5dB. Note that α is the ratio of the number of non-uniform samples given to NUSSB (for estimating the spectral support) to the number of uniform samples obtained at Nyquist rate. Based on the parameters estimated by NUSSB i.e. $\hat{N}_B$, $\hat{\mathcal{K}}$ in the adaptation phase, the DSB sampler selects the p non-uniform samples, corresponding to L uniform Nyquist samples, to operate in the reconstruction phase, see Fig.2. As the average sampling rate for the DSB sampler is $f_{avg} = (p/L)f_{Nyq}$, it can be seen that a false detection of $\hat{N}_B$, $\hat{\mathcal{K}}$ by NUSSB will directly effect the f_{avg} of the DSB sampler, as will be shown shortly.

The detection performance is evaluated by computing the probability of detecting the signal occupancy in terms of the number of bands N_B and the active cells set $\mathcal{K}$ as follows:

$$\begin{aligned} P_{d(N_B)} &= \Pr\left(\hat{N}_B = N_B\right) \\ P_{d(\mathcal{K})} &= \Pr\left(\hat{\mathcal{K}} = \mathcal{K}\right) \end{aligned} \tag{8}$$

and the false alarm probability is computed as

$$\begin{aligned} P_{fa(N_B)} &= \Pr\left(\hat{N}_B > N_B\right) \\ P_{fa(\mathcal{K})} &= \Pr\left(|\hat{\mathcal{K}}| > |\mathcal{K}| \Big| \hat{\mathcal{K}} \subset \mathcal{K}\right) \end{aligned} \tag{9}$$

where $|\mathcal{K}|$ represents the cardinality of $\mathcal{K}$. The subscripts N_B and $\mathcal{K}$ are used to distinguish the probabilities for the number of bands and the active cells set, respectively. We present both the $P_{d(N_B)}$ and $P_{d(\mathcal{K})}$, as the correct detection of the active cells set is linked to the correct detection of N_B, see equations (5),(6), (7). In order to compute P_d and P_{fa}, we have performed 1000 iterations at various values of SNR and for different number of samples given to the NUSSB i.e. different α. It should be noted that results in Figs.(6-9) are plotted when the DSB sampler is operating in adaptation phase (switch in position 2, see Fig.1), to explicitly show the performance of the NUSSB.

In Fig.6, $P_{d(N_B)}$ and $P_{d(\mathcal{K})}$ are plotted against varying SNR for $\alpha = 0.4, 0.5$. It can be seen here that for α=0.4, after SNR=5dB, our proposed sensing method is able to detect the total bands and the occupied cells with high probability. At α=0.5, the performance has further increased and we are able to detect with high probability at an SNR=2dB. Fig.6 shows that the performance of the proposed sensing model depends on the number of non-uniform samples available to NUSSB. To show

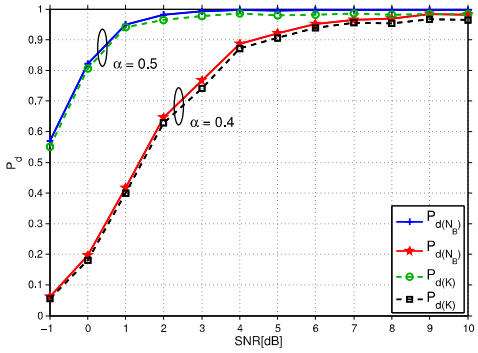

Fig. 6. $P_{fa(N_B)}$ and $P_{fa(\mathcal{K})}$ plotted against varying SNR for $\alpha = 0.4$ and $\alpha = 0.5$.

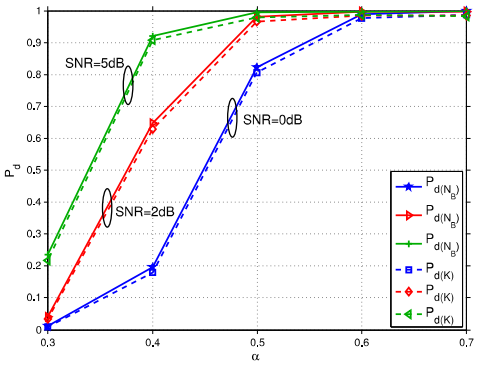

Fig. 7. $P_{d(N_B)}$, $P_{d(\mathcal{K})}$ plotted against varying α for different SNR.

this dependency, we have plotted $P_{d(N_B)}$ and $P_{d(\mathcal{K})}$ for varying values of α in Fig.7. It can be seen that the proposed sensing model behaves rather poorly at α=0.3 but its performance improves at α=0.4. At α=0.5, our proposed sensing model detects with high probability, approaching 1 after α =0.6.

Next in Fig.8, we plot the $P_{fa(N_B)}$ and $P_{fa(\mathcal{K})}$ as a function of varying SNR. At low SNR i.e. -1 dB, the values for $P_{fa(N_B)}$

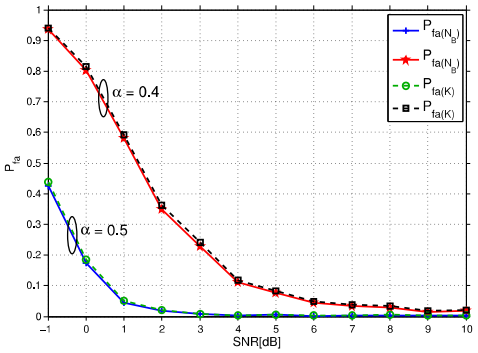

Fig. 8. $P_{fa(N_B)}$ and $P_{fa(\mathcal{K})}$ plotted against varying SNR for $\alpha = 0.4$ and $\alpha = 0.5$.

and $P_{fa(\mathcal{K})}$ are quite high, especially for α=0.4. But as the SNR increases, the $P_{fa(N_B)}$ and $P_{fa(\mathcal{K})}$ drop quickly, practically becoming zero at an SNR=3dB for α=0.5. As suspected, $P_{fa(N_B)}$ and $P_{fa(\mathcal{K})}$ also depend on the number of non-uniform samples available to NUSSB for detection. To show this, in Fig.9, we have plotted $P_{fa(N_B)}$ and $P_{fa(\mathcal{K})}$ for varying values of α at different SNR values. It can be seen that the performance of the

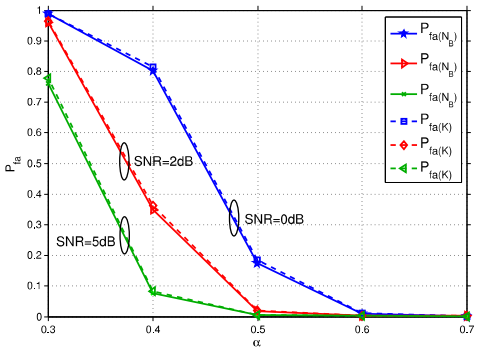

Fig. 9. $P_{fa(N_B)}$, $P_{fa(\mathcal{K})}$ plotted for varying α at different SNR.

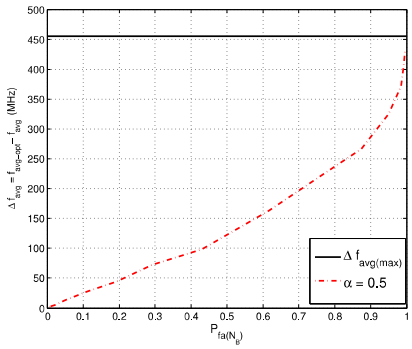

Fig. 11. Δf_{avg} is plotted against $P_{fa(N_B)}$ for α=0.5.

sensing model improves with increasing α.

As stated earlier, the probability of false alarm effects the averaging sampling rate f_{avg} of the DSB sampler. This happens because at a high P_{fa}, the NUSSB shows that the estimated spectral support $\mathcal{F}$ of the signal is larger than the actual support, as a result, the DSB sampler is forced to sample at a higher, unoptimized sampling rate. It should be noted that the results in Figs.10-11, show the impact of false detection (P_{fa}), performed in the adaptation phase, on the average sampling rate achieved in the reconstruction phase. To show this, in Fig.10, we have plotted average sampling rate $\hat{f}_{avg}$, achieved by DSB sampler based on the information received from NUSSB, against different values of α. In Fig.10, $f_{avg-opt}$, represents the optimal average sampling rate of DSB sampler when operating in non-blind mode i.e. having full information of the spectral support. When the DSB sampler operates in blind mode, $\hat{f}_{avg}$=f_{Nyq} represents the worst case and the ideal case is when $\hat{f}_{avg}$=$f_{avg-opt}$. The objective is that the difference Δf_{avg}=$(f_{avg-opt} - \hat{f}_{avg})$ must be zero. Fig.10 shows that for a given SNR, the $\hat{f}_{avg}$ ap-

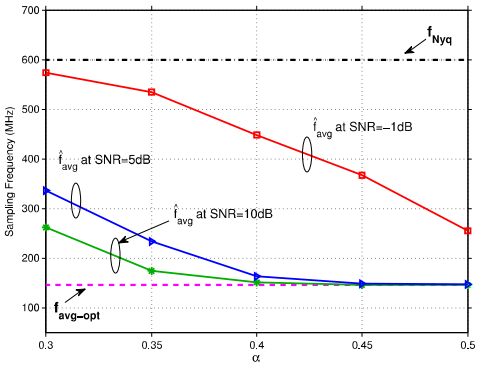

Fig. 10. Estimated average sampling rate $\hat{f}_{avg}$ of DSB sampler while operating in blind mode plotted against α.

proaches $f_{avg-opt}$ as α increases, which is normal, because for a given SNR, the P_{fa} of the NUSSB decreases with increase in α. This becomes more clear from Fig.11 where Δf_{avg} is plotted against $P_{fa(N_B)}$ for α= 0.5. It can be seen that with increase in $P_{fa(N_B)}$, Δf_{avg} increases and approaches the maximum Δf_{avg} at $P_{fa(N_B)}$=1. Note that here the maximum value for Δf_{avg}=$f_{Nyq} - f_{avg-opt}$ = 600-145 $\approx$ 455MHz. At low $P_{fa(N_B)}$ the proposed non-uniform spectrum sensing method works fine and the difference Δf_{avg} is close to zero.

5. CONCLUSION

In this paper, we have proposed a spectrum sensing technique based on non-uniform sub-Nyquist sampling. We have shown that the proposed sensing model works efficiently and shows high detection and low false alarm probabilities.The performance of the spectrum sensing model improves with increase in number of the non-uniform samples available to the sensing method. Finally, the effect of false detection is shown on the average sampling rate of the sampler.

6. REFERENCES

[1] Simon Haykin, "Cognitive radio: brain-empowered wireless communications," *Selected Areas in Communications, IEEE Journal on*, vol. 23, no. 2, pp. 201–220, 2005.

[2] Jacques Palicot and al, *Radio Engineering: from Software Radio to Cognitive Radio*, John Wiley Sons, June 2010.

[3] Yonghong Zeng, Ying-Chang Liang, Anh Tuan Hoang, and Rui Zhang, "A review on spectrum sensing for cognitive radio: challenges and solutions," *EURASIP J. Adv. Signal Process*, vol. 2010, pp. 2:2–2:2, Jan. 2010.

[4] Y.L. Polo, Ying Wang, A. Pandharipande, and G. Leus, "Compressive wide-band spectrum sensing," in *Acoustics, Speech and Signal Processing, 2009. ICASSP 2009. IEEE International Conference on*, April, pp. 2337–2340.

[5] Zhi Tian and G.B. Giannakis, "Compressed sensing for wideband cognitive radios," in *Acoustics, Speech and Signal Processing, 2007. ICASSP 2007. IEEE International Conference on*, April, vol. 4, pp. IV–1357–IV–1360.

[6] M. Rashidi, K. Haghighi, A. Owrang, and M. Viberg, "A wideband spectrum sensing method for cognitive radio using sub-nyquist sampling," in *Digital Signal Processing Workshop and IEEE Signal Processing Education Workshop (DSP/SPE), 2011 IEEE*, Jan., pp. 30–35.

[7] M. Rashidi, K. Haghighi, A. Panahi, and M. Viberg, "A nlls based sub-nyquist rate spectrum sensing for wideband cognitive radio," in *New Frontiers in Dynamic Spectrum Access Networks (DySPAN), 2011 IEEE Symposium on*, May, pp. 545–551.

[8] S. Traoré, B. Aziz, and D. Le Guennec, "Dynamic single branch non-uniform sampler," in *International Conference on Digital Signal Processing (DSP), Santorini, Greece*, 2013.

[9] Chiheb Rebai, Manel Ben-Romdhane, Patricia Desgreys, Patrick Loumeau, and Adel Ghazel, "Pseudorandom signal sampler for relaxed design of multistandard radio receiver," *Microelectronics Journal*, vol. 40, no. 6, pp. 991–999, 2009.

[10] S. Traoré, B. Aziz, D. Le Guennec, and J. Palicot, "Non-uniform sampling for spectral analysis of multi-band signals," in *2nd International Conference on Telecommunications and Remote Sensing Processing*, 2013.

[11] M. Rashidi Avendi, "Non-uniform sampling and reconstruction of multi-band signals and its application in wideband spectrum sensing of cognitive radio," 2010.

[12] J. D. Scargle, "Studies in astronomical time series analysis II. statistical aspects of spectral analysis of unevenly sampled data," *Astrophysical Journal*, vol. 263, pp. 835–853, 1982.